Materials Research Proceedings 31 (2023) 76-85 https://doi.org/10.21741/9781644902592-9

Static response of functionally graded porous spherical shells using trigonometric shear deformation theory

Rupali B. Tamnar[1,a *], Atteshamuddin S. Sayyad[2,b]

[1]Research Scholar, Department of Civil Engineering, Sanjivani College of Engineering, Savitribai Phule Pune University, Kopargaon-423603, Maharashtra, India

[2]Professor, Department of Structural Engineering, Sanjivani College of Engineering, Savitribai Phule Pune University, Kopargaon-423603, Maharashtra, India

[a]tamnar1991@gmail.com, [b]attu_sayyad@yahoo.co.in

Keywords: Trigonometric Shear Deformation Theory, Functionally Graded Shells, Porosity, Static Response

Abstract. In this study, a static response of FGM shells containing even distribution of porosity is investigated using a trigonometric shear deformation theory accounts for effects of transverse shear and normal strains. The principal of virtual work is used for obtaining governing equations and boundary conditions of the current theory. The theory satisfies zero transverse shear stress conditions at the top and the bottom surfaces of the shell. The simply-supported FGM shell is analyzed in the present study using the Navier method. The present results of displacements and stresses in FGM shells are obtained and compared with other higher order theories available in the literature to verify the current theory.

Introduction

Functionally graded materials (FGMs) is a new class of material which has many applications in the field of aerospace, civil, mechanical, biomedical, chemical, nuclear, mining, and power plant industries. Functionally graded materials has many advantages such as smooth stress distribution, less stress concentration and high joint strength of different materials. The porosities inside FGM can occur during the fabrication and lead to occurrence of micro-voids in the material and therefore reduction the density of the material and ultimately strength of the material. Therefore, many researchers have worked on static problems of FGM shells considering the effects of porosity. Kirchhoff [1] and Mindlin [2] have developed the classical shell theory (CST) and the first-order shear deformation theory (FSDT) respectively for the analysis of shear deformable beams, plates, and shells. But these theories are assumption based theories, and not appropriate for the accurate analysis of thick plates/shells made up of advanced composite materials such as FGM. Therefore, researchers have developed refined higher-order shell theories which capture the bending behaviour accurately and predicts safe design of the composite shells. Sayyad and Ghugal [3] have presented static and free vibration analysis of FGM shells with double curvature using various types of higher-order shell theories uisng a generalized shear deformation theory. Shinde and Sayyad [4, 5] have developed a new fifth-order shear and normal deformation theory for the static and vibration analysis of FGM sandwich plates and shells. Yan and Zu [6] focused on the large amplitude vibration of sigmoid functionally graded materials thin plates with porosities. Wattanasakulpong and Ungbhakorn [7] studied the vibration properties of FGM porous beams using the differential transformation approach with various types of elastic supports. Yan and Zu [8] have studied the vibration behaviors of rectangular FGM plates with porosities and moving in thermal environment.Wang et al. [9] performed the vibration analysis of longitudinal traveling FGM porous plates considering even and uneven porosity distributions. Zhu et al. [10] presented the static and dynamic responses of functionally graded material pipes with porosities and

Materials Research Proceedings 31 (2023) 76-85 https://doi.org/10.21741/9781644902592-9

geometric imperfections. Zenkour [11] studied the generalized shear deformation theory for bending analysis of functionally graded plates. Dharan et al. [12] studied a higher order shear deformation model for functionally graded plates. Hadji et al. [13] performed bending and free vibration analysis for FGM plates containing various distribution shapes of porosity.

Geometric configuration and material properties

For the sake of theoretical formulation, a spherical shell element on a rectangular platform in the Cartesian coordinate system (*x, y, z*) is taken into consideration. A shell has thickness *h* in the *z*-direction and curved dimensions *a* and *b* in the *x* and *y* directions, respectively. The principle radii of curvature along the *x* and *y* axes of the mid-plane are represented by R_1 and R_2, respectively. The transverse load *q* (*x, y*) is applied to the upper surface of the shell i.e. $z = -h/2$.

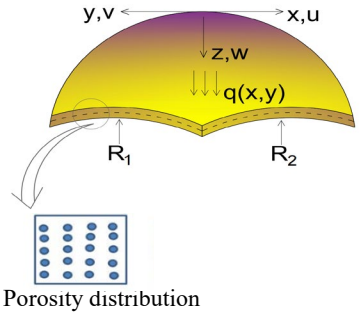

Fig 1. Geometric configuration and porosity distribution of FGM shells

In this study, the authors have considered an FGM shell with the homogenous porosity distribution ((α < < 1). The modified mixture rule proposed by Wattanasakulpong and Ungbhakornb [7] is as follows.

$$P(z) = (P_c - P_m)\left(\frac{z}{h} + \frac{1}{2}\right)^p + P_m - (P_c + P_m)\frac{\alpha}{2}. \quad (1)$$

where, *P*(*z*) represents the material properties, p is the power-law index that takes values greater than or equals to zero; α is the porosity distribution factor. The FGM shell becomes a fully ceramic when $p = 0$ and fully metal when $p = \infty$. The FGM shell is called perfect when $\alpha = 0$ and imperfect when $\alpha \neq 0$. The Eq. (1) for the modulus of elasticity of the material is modified as.

$$E(z) = (E_c - E_m)\left(\frac{z}{h} + \frac{1}{2}\right)^p + E_m - (E_c + E_m)\frac{\alpha}{2}. \quad (2)$$

Development of theory

The displacement field of the current trigonometric shear deformation theory for the FGM shell is as follows.

$$\begin{aligned} u(x,y,z) &= \left(1 + \frac{z}{R_1}\right) u_0(x,y) - z\frac{\partial w_0}{\partial x} + \frac{h}{\pi}\sin\left(\frac{\pi z}{h}\right)\theta_x \\ v(x,y,z) &= \left(1 + \frac{z}{R_2}\right) v_0(x,y) - z\frac{\partial w_0}{\partial y} + \frac{h}{\pi}\sin\left(\frac{\pi z}{h}\right)\theta_y \\ w(x,y,z) &= w_0(x,y) + c_1 cos\left(\frac{\pi z}{h}\right)\theta_z. \end{aligned} \quad (3)$$

where *u, v, w* are the displacements of any point of the shell in *x, y, z* directions respectively; (u_0, v_0, w_0) are the mid-plane displacements in *x, y, z* directions; $(\theta_x, \theta_y, \theta_z)$ are the shear rotations; $\frac{h}{\pi} sin\frac{\pi z}{h}$ represent the shape function associated with the realistic distribution of transverse shear strain across the thickness of the shell; c_1 is the arbitrary constant included to consider or not to consider the effects of transverse normal strain. Using the linear theory of

elasticity, the normal and shear strains associated with the current theory are obtained

$$\varepsilon_x = \left(\frac{\partial u_0}{\partial x} + \frac{w_0}{R_1}\right) - z\frac{\partial^2 w_0}{\partial x^2} + f(z)\frac{\partial \theta_x}{\partial x} + C_1\frac{f'(z)}{R_1}\theta_z$$
$$\varepsilon_y = \left(\frac{\partial v_0}{\partial y} + \frac{w_0}{R_2}\right) - z\frac{\partial^2 w_0}{\partial y^2} + f(z)\frac{\partial \theta_y}{\partial y} + C_1\frac{f'(z)}{R_2}\theta_z$$
$$\varepsilon_z = c_1 f''(z)\theta_z$$
$$\gamma_{xy} = \frac{\partial u_0}{\partial y} + \frac{\partial v_0}{\partial x} - 2z\frac{\partial^2 w_0}{\partial x \partial y} + f(z)\left(\frac{\partial \theta_x}{\partial y} + \frac{\partial \theta_y}{\partial x}\right) \quad (4)$$
$$\gamma_{xz} = f'(z)\theta_x + f'(z)\frac{\partial \theta_x}{\partial x}$$
$$\gamma_{yz} = f'(z)\theta_y + f'(z)\frac{\partial \theta_z}{\partial y}.$$

where

$$f(z) = \frac{h}{\pi}\sin\left(\frac{\pi z}{h}\right),\ f'(z) = \cos\left(\frac{\pi z}{h}\right),\ f''(z) = -\sin\left(\frac{\pi z}{h}\right)\left(\frac{\pi}{h}\right). \quad (5)$$

The following Hooke's law is used to calculate the normal and transverse stresses of the FGM shell.

$$\begin{Bmatrix}\sigma_x\\ \sigma_y\\ \sigma_z\\ \tau_{xy}\\ \tau_{xz}\\ \tau_{yz}\end{Bmatrix} = \begin{bmatrix}Q_{11} & Q_{12} & Q_{13} & 0 & 0 & 0\\ Q_{12} & Q_{22} & Q_{23} & 0 & 0 & 0\\ Q_{13} & Q_{23} & Q_{33} & 0 & 0 & 0\\ 0 & 0 & 0 & Q_{66} & 0 & 0\\ 0 & 0 & 0 & 0 & Q_{44} & 0\\ 0 & 0 & 0 & 0 & 0 & Q_{55}\end{bmatrix}\begin{Bmatrix}\varepsilon_x\\ \varepsilon_y\\ \varepsilon_z\\ \gamma_{xy}\\ \gamma_{xz}\\ \gamma_{yz}\end{Bmatrix} \quad (6)$$

where $(\sigma_x, \sigma_y, \sigma_z, \tau_{xy}, \tau_{xz}, \tau_{yz})$ represent the normal and shear stresses, $(\varepsilon_x, \varepsilon_y, \varepsilon_z, \gamma_{xy}, \gamma_{yz}, \gamma_{xz})$ represent the normal and shear strains, and Q_{ij} represents the reduced stiffness coefficients.

where

$$Q_{11} = Q_{22} = Q_{33} = \left(\frac{E(1-\mu)}{(1+\mu)(1-2\mu)}\right)$$
$$Q_{12} = Q_{13} = Q_{23} = Q_{21} = Q_{31} = Q_{32} = \frac{\mu}{(1-\mu)}\left(\frac{E(1-\mu)}{(1+\mu)(1-2\mu)}\right) \quad (7)$$
$$Q_{44} = Q_{55} = Q_{66} = \frac{1-2\mu}{2(1-\mu)}\left(\frac{E(1-\mu)}{(1+\mu)(1-2\mu)}\right).$$

The governing equations of the current trigonometric theory are derived by using the principle of virtual work.

$$\int_0^a \int_0^b \int_{-h/2}^{h/2} \left(\sigma_x \delta\varepsilon_x + \sigma_y \delta\varepsilon_y + \sigma_z \delta\varepsilon_z + \tau_{xy}\delta\gamma_{xy} + \tau_{xz}\delta\gamma_{xz} + \tau_{yz}\delta\gamma_{yz}\right) dx\, dy\, dz -$$
$$\int_0^a \int_0^b q(x,y)\,\delta w\, dx\, dy = 0 \quad (8)$$

Substituting the values of strains and stresses from Eq. (4) and Eq. (6) into Eq. (8), integrating Eq. (8) by parts and collecting the coefficients of unknown variables, the following six governing equations are derived.

$$\delta u_0: A_{12}\left(\frac{\partial^2 u_0}{\partial x^2} + \frac{1}{R_1}\frac{\partial w_0}{\partial x}\right) - B_{11}\frac{\partial^3 w_0}{\partial x^3} + C_{11}\frac{\partial^2 \theta_x}{\partial x^2} + A_{12}\left(\frac{\partial^2 v_0}{\partial x\,\partial y} + \frac{1}{R_1}\frac{\partial w_0}{\partial x}\right) - B_{12}\frac{\partial^2 w_0}{\partial x\,\partial y^2}$$
$$+\left(\frac{f_{11}}{R_1} + \frac{f_{12}}{R_2}\right)c_1\frac{\partial \theta_z}{\partial x} + c_{12}\frac{\partial^2 \theta_y}{\partial x\,\partial y} + D_{13}\,c_1\frac{\partial \theta_z}{\partial x} + A_{66}\left(\frac{\partial^2 u_0}{\partial y^2} + \frac{\partial^2 v_0}{\partial x^2}\right) - 2\,B_{66}\frac{\partial^3 w_0}{\partial x\,\partial y^2} + C_{66}\left(\frac{\partial^2 \theta_x}{\partial y^2} + \frac{\partial^2 \theta_y}{\partial x\,\partial y}\right) \quad (9)$$

$$\delta v_0: A_{21}\left(\frac{\partial^2 u_0}{\partial x\,\partial y} + \frac{1}{R_1}\frac{\partial w_0}{\partial y}\right) - B_{21}\frac{\partial^3 w_0}{\partial x^2\,\partial y} + C_{21}\frac{\partial^2 \theta_x}{\partial x\,\partial y} + A_{22}\left(\frac{\partial^2 v_0}{\partial y^2} + \frac{1}{R_2}\frac{\partial w_0}{\partial y}\right) - B_{22}\frac{\partial^3 w_0}{\partial y^3} +$$
$$\left(\frac{F_{21}}{R_1} + \frac{F_{22}}{R_2}\right)c_1\frac{\partial \theta_z}{\partial y} + c_{22}\frac{\partial^2 \theta_y}{\partial y^2} + D_{23}\,c_1\frac{\partial \theta_z}{\partial y} + A_{66}\left(\frac{\partial^2 u_0}{\partial x\,\partial y} + \frac{\partial^2 v_0}{\partial x^2}\right) - 2\,B_{66}\frac{\partial^3 w_0}{\partial x^2\,\partial y} + C_{66}\left(\frac{\partial^2 \theta_x}{\partial x\,\partial y} + \frac{\partial^2 \theta_y}{\partial x^2}\right) \quad (10)$$

$$\partial w_0: B_{11}\left(\frac{\partial^3 u_0}{\partial x^3}+\frac{1}{R_1}\frac{\partial^2 w_0}{\partial x^2}\right)-H_{11}\frac{\partial^4 w_0}{\partial x^4}+I_{11}\frac{\partial^3 \theta_x}{\partial x^3}+\left(\frac{J_{11}}{R_1}+\frac{J_{12}}{R_2}\right)c_1\frac{\partial^2 \theta_z}{\partial x^2}$$
$$+B_{12}\left(\frac{\partial^3 v_0}{\partial x^2\partial y}+\frac{1}{R_2}\frac{\partial^2 w_0}{\partial x^2}\right)-H_{12}\frac{\partial^4 w_0}{\partial x^2\partial y^2}+I_{12}\frac{\partial^3 \theta_y}{\partial x^2\partial y}+K_{13}c_1\frac{\partial^2 \theta_z}{\partial x^2}+B_{21}\frac{\partial^3 u_0}{\partial x\,\partial y^2}-H_{21}\frac{\partial^4 w_0}{\partial x^2\,\partial y^2}$$
$$+I_{21}\frac{\partial^3 \theta_x}{\partial x\,\partial y^2}+B_{21}\frac{1}{R_1}\frac{\partial^2 w_0}{\partial y^2}+J_{21}\frac{c_1}{R_1}\frac{\partial^2 \theta_z}{\partial y^2}+B_{22}\frac{\partial^3 v_0}{\partial y^3}-H_{22}\frac{\partial^4 w_0}{\partial y^4}+I_{22}\frac{\partial^3 \theta_y}{\partial y^3}+B_{22}\frac{1}{R_2}\frac{\partial^2 w_0}{\partial y^2}$$
$$+J_{22}\frac{c_1}{R_2}\frac{\partial^2 \theta_z}{\partial y^2}+K_{23}c_1\frac{\partial^2 \theta_z}{\partial y^2}+2B_{66}\frac{\partial^3 u_0}{\partial x\,\partial y^2}+2B_{66}\frac{\partial^3 v_0}{\partial x^2\,\partial y}-4H_{66}2B_{66}\frac{\partial^4 w_0}{\partial x^2\,\partial y^2}+2C_{66}\frac{\partial^3 \theta_x}{\partial x\partial y^2}$$
$$+2C_{66}\frac{\partial^3 \theta_y}{\partial x^2\partial y}+\left(-\frac{A_{11}}{R_1}\left(\frac{\partial u_0}{\partial x}+\frac{w_0}{R_1}\right)\right)+\frac{B_{11}}{R_1}\frac{\partial^2 w_0}{\partial x^2}-\frac{C_{11}}{R_1}\frac{\partial \theta_x}{\partial x}-\frac{1}{R_1}\left(\frac{F_{11}}{R_1}+\frac{F_{12}}{R_2}\right)c_1\theta_z-$$
$$\frac{A_{12}}{R_1}\left(\frac{\partial v_0}{\partial y}+\frac{w_0}{R_2}\right)+\frac{B_{12}}{R_1}\frac{\partial^2 w_0}{\partial y^2}-\frac{C_{12}}{R_1}\frac{\partial \theta_y}{\partial y}-\frac{D_{13}}{R_1}c_1\theta_z+\left(-\frac{A_{21}}{R_1}\left(\frac{\partial u_0}{\partial x}+\frac{w_0}{R_1}\right)\right)+\frac{B_{21}}{R_2}\frac{\partial^2 w_0}{\partial x^2}$$
$$-\frac{C_{21}}{R_2}\frac{\partial \theta_x}{\partial x}-\frac{1}{R_2}\left(\frac{F_{21}}{R_1}+\frac{F_{22}}{R_2}\right)c_1\theta_z-\frac{A_{22}}{R_2}\left(\frac{\partial v_0}{\partial y}+\frac{w_0}{R_2}\right)+\frac{B_{22}}{R_2}\frac{\partial^2 w_0}{\partial y^2}-\frac{C_{22}}{R_2}\frac{\partial \theta_y}{\partial y}-\frac{D_{23}}{R_2}c_1\theta_z=-q \tag{11}$$

$$\delta\theta_x: C_{11}\left(\frac{\partial^2 u_0}{\partial x^2}+\frac{1}{R_1}\frac{\partial w_0}{\partial x}\right)-I_{11}\frac{\partial^2 w_0}{\partial x^3}+L_{11}\frac{\partial^2 \theta_x}{\partial x^2}+C_{12}\left(\frac{\partial^2 v_0}{\partial x\partial y}+\frac{1}{R_2}\frac{\partial w_0}{\partial x}\right)-I_{12}\frac{\partial^3 w_0}{\partial x\partial y^2}$$
$$+L_{12}\frac{\partial^2 \theta_y}{\partial x\,\partial y}+N_{13}\frac{\partial \theta_z}{\partial x}+C_{66}\left(\frac{\partial^2 u_0}{\partial y^2}+\frac{\partial^2 v_0}{\partial x\partial y}\right)-2I_{66}\frac{\partial^3 w_0}{\partial x\,\partial y^2}+C_{66}\left(\frac{\partial^2 \theta_x}{\partial y^2}+\frac{\partial^2 \theta_y}{\partial x\partial y}\right)-$$
$$O_{55}\theta_x-O_{55}\frac{\partial \theta_z}{\partial x}+\frac{\partial \theta_z}{\partial x}\left(\frac{M_{11}}{R_1}+\frac{M_{12}}{R_2}\right)-\frac{F_{55}}{R_1}u_0=0 \tag{12}$$

$$\delta\theta_y: C_{21}\left(\frac{\partial^2 u_0}{\partial x\,\partial y}+\frac{1}{R_1}\frac{\partial w_0}{\partial y}\right)-I_{21}\frac{\partial^3 w_0}{\partial x^2\partial y}+L_{21}\frac{\partial^2 \theta_x}{\partial x\partial y}+C_{22}\left(\frac{\partial^2 v_0}{\partial y^2}+\frac{1}{R_2}\frac{\partial w_0}{\partial y}\right)-I_{22}\frac{\partial^3 w_0}{\partial y^3}$$
$$+\frac{\partial \theta_z}{\partial y}\left(\frac{M_{21}}{R_1}+\frac{M_{22}}{R_2}\right)c_1+L_{12}\frac{\partial^2 \theta_y}{\partial y^2}+N_{23}c_1\frac{\partial \theta_z}{\partial y}+C_{66}\left(\frac{\partial^2 u_0}{\partial x\partial y}+\frac{\partial^2 v_0}{\partial x^2}\right)-2I_{66}\frac{\partial^3 w_0}{\partial x^2\,\partial y}$$
$$+L_{66}\left(\frac{\partial^2 \theta_x}{\partial x\,\partial y}+\frac{\partial^2 \theta_y}{\partial x^2}\right)-O_{44}\theta_y-O_{44}c_1\frac{\partial \theta_z}{\partial y}=0 \tag{13}$$

$$\delta\theta_z: O_{55}\left(\frac{\partial \theta_x}{\partial x}c_1+c_1^2\frac{\partial \theta_z}{\partial x^2}\right)+O_{44}\left(\frac{\partial \theta_y}{\partial y}c_1+c_1^2\frac{\partial \theta_z}{\partial y^2}\right)+\left(-\frac{F_{11}}{R_1}c_1\left(\frac{\partial u_0}{\partial x}+\frac{w_0}{R_1}\right)\right)+\frac{J_{11}}{R_1}c_1\frac{\partial^2 w_0}{\partial x^2}$$
$$-\frac{M_{11}}{R_1}c_1\frac{\partial \theta_x}{\partial x}-\frac{F_{12}}{R_1}c_1\left(\frac{\partial v_0}{\partial y}+\frac{w_0}{R_2}\right)+\frac{J_{12}}{R_1}c_1\frac{\partial^2 w_0}{\partial y^2}-\frac{1}{R_1}\left(\frac{O_{11}}{R_1}+\frac{O_{12}}{R_2}\right)c_1^2\theta_z-\frac{M_{12}}{R_1}c_1\frac{\partial \theta_y}{\partial y}$$
$$-\frac{P_{13}}{R_1}c_1^2\theta_z-\frac{M_{22}}{R_2}c_1\frac{\partial \theta_y}{\partial y}-\frac{P_{23}}{R_2}c_1^2\theta_z+\left(-D_{13}c_1\left(\frac{\partial u_0}{\partial x}+\frac{w_0}{R_1}\right)\right)+K_{31}c_1\frac{\partial^2 w_0}{\partial x^2}-N_{31}c_1\frac{\partial \theta_x}{\partial x}$$
$$-D_{32}c_1\left(\frac{\partial v_0}{\partial y}+\frac{w_0}{R_2}\right)+K_{32}c_1\frac{\partial^2 w_0}{\partial y^2}-\left(\frac{P_{31}}{R_1}+\frac{P_{32}}{R_2}\right)c_1^2\theta_z-N_{32}c_1\frac{\partial \theta_y}{\partial y}-S_{33}c_1^2\theta_z=0 \tag{14}$$

where

$$\left(A_{ij},\ B_{ij}, HH_{ij}, C_{ij}, F_{ij}\ I_{ij}\right)=Q_{ij}\int_{-h/2}^{h/2}[1,\ z, z^2, f(z), f'(z), zf(z)]\,dz,$$
$$\left(L_{ij}\right)=Q_{ij}\int_{-h/2}^{h/2}\{[f(z)]^2\}\ dz, \left(O_{ij}\right)=Q_{ij}\int_{-h/2}^{h/2}[f'(z)]^2\,dz,$$
$$\left(D_{ij}, S_{ij}, P_{ij}\right)=Q_{ij}\int_{-h/2}^{h/2}\{f''(z), [f''(z)]^2, [f''(z)f'(z)]\}\,dz,$$
$$\left(KK_{ij},\ N_{ij}\right)=Q_{ij}\int_{-h/2}^{h/2}f''(z)[z, f(z)]\,dz, \text{ and } \left(J_{ij},\ M_{ij}\right)=Q_{ij}\int_{-h/2}^{h/2}f'(z)[z, f(z)]\ dz \tag{15}$$

Static analysis using the Navier method

According to the literature, the Navier method is the simplest and most popularly used semi-analytical method for the analysis of simply-supported boundary conditions of FGM shell. As per the assumption in the Navier method, the following solution form for the unknown variables is assumed which satisfying the simply-supported boundary conditions exactly.

$$(u_0,\ \theta_x)=(u_{mn},\ \theta_{xmn})\cos\lambda x\ \sin\beta y$$

$$(v_0,\ \theta_y) = (v_{mn},\ \theta_{ymn})\sin\lambda x\ \cos\beta y \quad (16)$$
$$(w_0,\ \theta_z) = (w_{mn},\ \theta_{zmn})\sin\lambda x\ \sin\beta y.$$

where $u_{mn,}\ v_{mn,}\ w_{mn,}\ \theta_{xmn,}\ \theta_{ymn,}\ \theta_{zmn,}$ are the unknown coefficients to be determine; $\lambda = \frac{m\pi}{a}, \beta = \frac{n\pi}{b}$. The expression for the transverse sinusoidal load is expressed as.

$$q(x,y) = q_0 \sin\lambda x \sin\beta y. \quad (17)$$

where q_0 is Fourier coefficient of load. Substitution of Eqs. (16) and (17) into Eqs. (9) – (14) leads to the six simultaneous equations which are written in the following matrix form.

$$[K]\{\Delta\} = \{f\} \quad (18)$$

where $[K]$ is the stiffness matrix, $\{f\}$ is the force vector and $\{\Delta\}$ is the vector of unknowns.

Numerical Result and Discussion

In this study, static analysis of simply-supported FGM porous shell is presented using the trigonometric shear deformation theory. The effects of homogenous porosity distribution on the static response of FGM shell are investigated. In order to verify the current theory, comparisons of the present results are done with those available in the literature. A FGM shell is made up of the following material.

Metal (Aluminium, Al): $E_m = 70\ GPa$,μ=0.3$E_m = 70\ GPa$

Ceramic (Alumina, Al_2O_3): $E_c = 380\ GPa$, μ=0.3

The numerical results are presented in the following dimensionless form for the comparison purpose.

$$\bar{w} = 10\ \frac{E_c h^3}{q_0\, a^4} w\left(\frac{a}{2},\frac{b}{2}\right),\ \bar{u} = 10\ 0\ \frac{E_c h^3}{q_0\, a^4} u\left(0,\frac{b}{2},\frac{-h}{4}\right),\ \bar{v} = 10\ 0\ \frac{E_c h^3}{q_0\, a^4} w\left(\frac{a}{2},0,\frac{-h}{6}\right)$$
$$\bar{\sigma}_x = \frac{h}{aq_0}\sigma_x\left(\frac{a}{2},\frac{b}{2},\frac{h}{2}\right),\ \bar{\sigma}_y = \frac{h}{aq_0}\sigma_y\left(\frac{a}{2},\frac{b}{2},\frac{h}{3}\right), \quad (19)$$
$$\bar{\tau}_{xz} = \frac{h}{aq_0}\tau_{xz}\left(0,\frac{b}{2},0\right),\ \bar{\tau}_{yz} = \frac{h}{aq_0}\tau_{yz}\left(\frac{a}{2},0,\frac{h}{6}\right).$$

Table 1 shows the comparison of in-plane and transverse displacements of FGM plates and porous shells subjected to sinusoidal load. Table 1 examine the effects of the power-law index and the porosity distribution factor on the dimensionless displacements. Table 1 reveals that the increase in the power-law index and the porosity distribution factor increases the values of dimensionless displacements. The present theory is in close agreement with the existing literature. Fig. 2 plots through-the-thickness variations of in-plane displacements for different values of the power-law index and the porosity distribution factor. Table 2 shows comparison of in-plane normal stresses of FGM plates and porous shells subjected to sinusoidal loading. Examination of Table 2 shows that increase in the values of the power-law index and the porosity factor also increases the values of dimensionless in-plane stresses. Fig. 3 shows through-the-thickness distributions of in-plane stresses in FGM porous shells for different power-law index whereas Fig. 4 shows through-the-thickness distributions of in-plane stresses in FGM porous shells for different porosity distribution factors.

Table 1 Effects of the power-law index and the porosity distribution factor on the dimensionless

			Plate (R_1=R_2 =∞)		Spherical Shells (R_1=R_2 =R)	
p	Theory	α	$\overline{u}$	$\overline{w}$	$\overline{u}$	$\overline{w}$
0	Present	$\alpha = 0$	0.21810	0.29603	0.20586	0.77894
		$\alpha = 0.1$	0.23150	0.31710	0.23152	0.20951
		$\alpha = 0.2$	0.24651	0.34265	0.23323	0.90182
	Hadji et al. [13]	$\alpha = 0$	0.21816	0.29604	-	-
		$\alpha = 0.1$	0.23189	0.31468	-	-
		$\alpha = 0.2$	0.24746	0.33581	-	-
	Dharan et al. [12]	$\alpha = 0$	0.21805	0.29423	-	-
	Zenkour [11]	$\alpha = 0$	0.23090	0.29600	-	-
1	Present	$\alpha = 0$	0.64097	0.58810	0.40649	0.34539
		$\alpha = 0.1$	0.77030	0.68758	0.46073	0.38848
		$\alpha = 0.2$	0.96276	0.85487	0.53045	0.44553
	Hadji et al. [13]	$\alpha = 0$	0.64112	0.58893	-	-
		$\alpha = 0.1$	0.77156	0.68318	-	-
		$\alpha = 0.2$	0.96748	0.81924	-	-
	Dharan et al. [12]	$\alpha = 0$	0.64258	0.59059	-	-
	Zenkour [11]	$\alpha = 0$	0.66260	0.58890	-	-
2	Present	$\alpha = 0$	0.89746	0.75714	0.54258	1.99248
		$\alpha = 0.1$	1.18013	0.96435	0.64490	0.52566
		$\alpha = 0.2$	1.69307	1.51949	0.77297	0.65214
	Hadji et al. [13]	$\alpha = 0$	0.89793	0.75733	-	-
		$\alpha = 0.1$	1.18383	0.94196	-	-
		$\alpha = 0.2$	1.73521	1.28005	-	-
	Dharan et al. [12]	$\alpha = 0$	0.90220	0.76697	-	-
	Zenkour [11]	$\alpha = 0$	0.92810	0.75730	-	-
5	Present	$\alpha = 0$	1.06620	0.91216	0.73865	2.40040
		$\alpha = 0.1$	1.50131	1.34216	0.93113	3.53200
		$\alpha = 0.2$	2.77676	1.65803	1.40101	4.36323
	Hadji et al. [13]	$\alpha = 0$	1.06620	0.91171	-	-
		$\alpha = 0.1$	1.52547	1.19970	-	-
		$\alpha = 0.2$	2.70313	1.87542	-	-
	Dharan et al. [12]	$\alpha = 0$	1.06786	0.94325	-	-
	Zenkour [11]	$\alpha = 0$	1.11580	0.91180	-	-

displacements of a FGM plates and shells subjected to sinusoidal loading (a/h = 10, R/a = 1)

Table 2 Effects of the power-law index and the porosity distribution factor on the dimensionless in-plane normal stresses of a FGM plates and shells subjected to sinusoidal loading (a/h = 10, R/a = 1)

			Plate (R_1=R_2 =∞)		Spherical Shells (R_1=R_2 =R)	
p	Theory	α	$\bar{\sigma}_x$	$\bar{\sigma}_y$	$\bar{\sigma}_x$	$\bar{\sigma}_y$
0	Present	$\alpha = 0$	1.99370	1.31090	0.87764	0.04216
		$\alpha = 0.1$	1.99700	1.31040	0.87618	0.04506
		$\alpha = 0.2$	2.00150	1.30920	0.87391	0.04956
	Hadji et al. [13]	$\alpha = 0$	1.99515	1.31219	-	-
		$\alpha = 0.1$	1.99515	1.31219	-	-
		$\alpha = 0.2$	1.99515	1.31219	-	-
	Dharan et al. [12]	$\alpha = 0$	1.98915	1.31035	-	-
	Zenkour [11]	$\alpha = 0$	1.99550	1.31210	-	-
1	Present	$\alpha = 0$	3.27700	1.31090	1.34432	0.04290
		$\alpha = 0.1$	3.27130	1.51480	1.39291	0.04330
		$\alpha = 0.2$	3.55570	1.55050	1.45108	0.03950
	Hadji et al. [13]	$\alpha = 0$	3.08640	1.48950	-	-
		$\alpha = 0.1$	3.26288	1.51850	-	-
		$\alpha = 0.2$	3.51847	1.56040	-	-
	Dharan et al. [12]	$\alpha = 0$	3.07011	1.48935	-	-
	Zenkour [11]	$\alpha = 0$	3.08700	1.48940	-	-
2	Present	$\alpha = 0$	3.60550	1.38750	1.66029	0.05110
		$\alpha = 0.1$	3.99110	1.41052	1.76702	0.04740
		$\alpha = 0.2$	4.86129	1.44234	1.88560	0.05180
	Hadji et al. [13]	$\alpha = 0$	3.60856	1.39575	-	-
		$\alpha = 0.1$	3.96831	1.41036	-	-
		$\alpha = 0.2$	4.61670	1.43564	-	-
	Dharan et al. [12]	$\alpha = 0$	3.58089	1.39680	-	-
	Zenkour [11]	$\alpha = 0$	3.60940	1.39540	-	-
5	Present	$\alpha = 0$	4.24726	1.06810	2.24739	0.03880
		$\alpha = 0.1$	4.88748	1.01340	2.48838	0.03880
		$\alpha = 0.2$	5.60382	0.94690	2.97257	0.03970
	Hadji et al. [13]	$\alpha = 0$	4.24758	1.10329	-	-
		$\alpha = 0.1$	4.74916	1.03851	-	-
		$\alpha = 0.2$	5.78994	0.88676	-	-
	Dharan et al. [12]	$\alpha = 0$	4.19547	1.10870	-	-
	Zenkour [11]	$\alpha = 0$	4.24880	1.10290	-	-

Materials Research Proceedings 31 (2023) 76-85 https://doi.org/10.21741/9781644902592-9

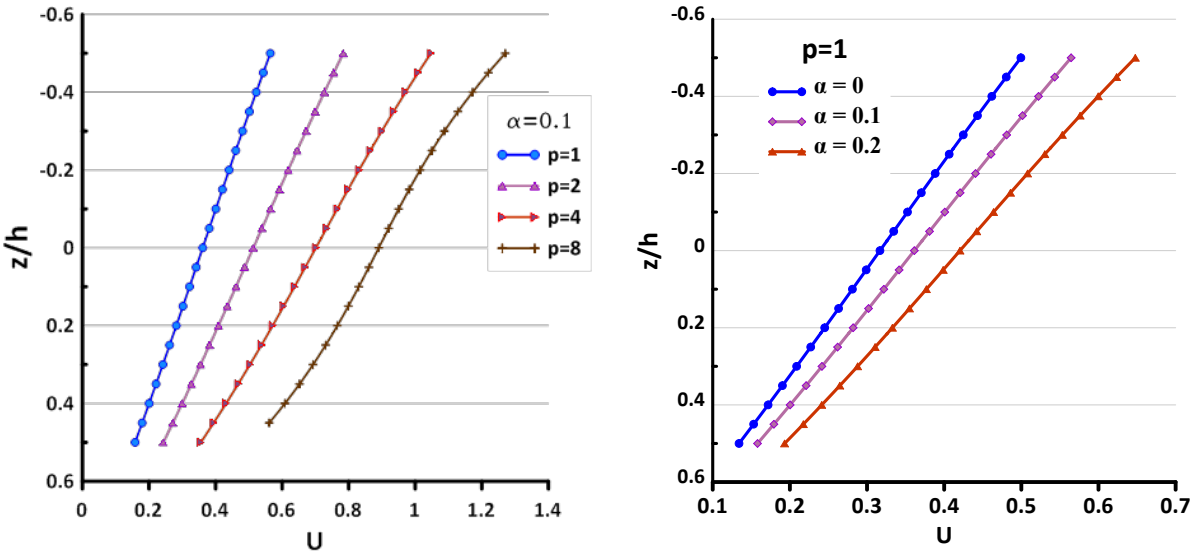

Fig. 2. Effects of the power-law index and the porosity distribution factor on the in-plane displacement of FGM spherical shell (*a/h*=10, *R/a*=1)

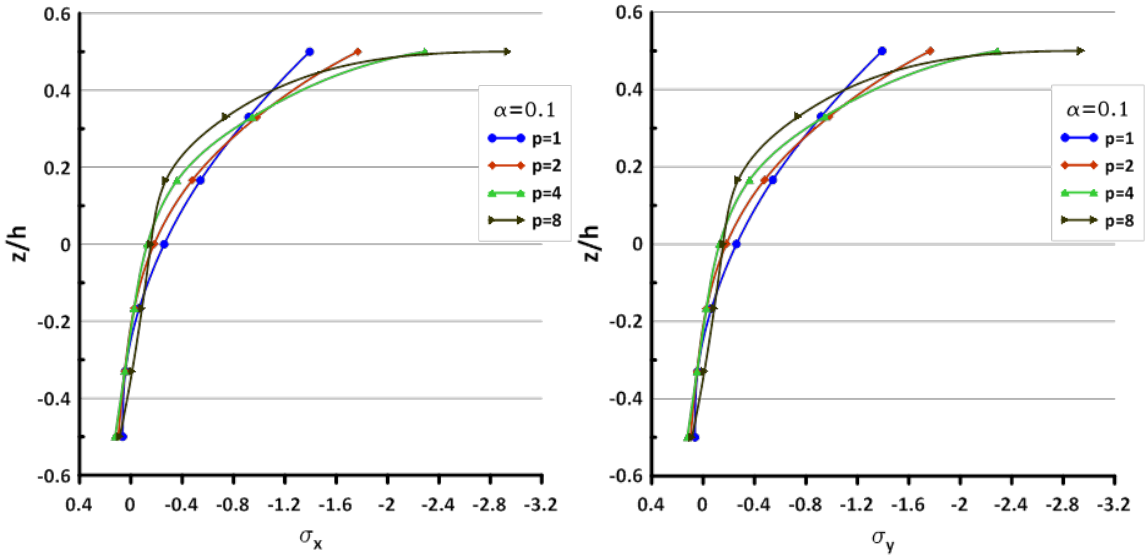

Fig. 3. Effects of the power-law index on the through-the-thickness distributions of in-plane normal stresses for FGM spherical shell (a/h=10, R/a=1).

Conclusions

This paper focused on investigating a static response of FGM porous shells using a trigonometric shear deformation theory accounts for effects of transverse shear and normal strains. The simply-supported FGM shell is analyzed in the present study using the Navier method. Based on the numerical results and the discussion it is concluded that the present theory is accurate enough to capture the static bending response of FGM shells with homogenous porosity effects. It is also concluded that the values of dimensionless displacements and in-plane stresses are directly proportional to the power-law index as well as the porosity distribution factor.

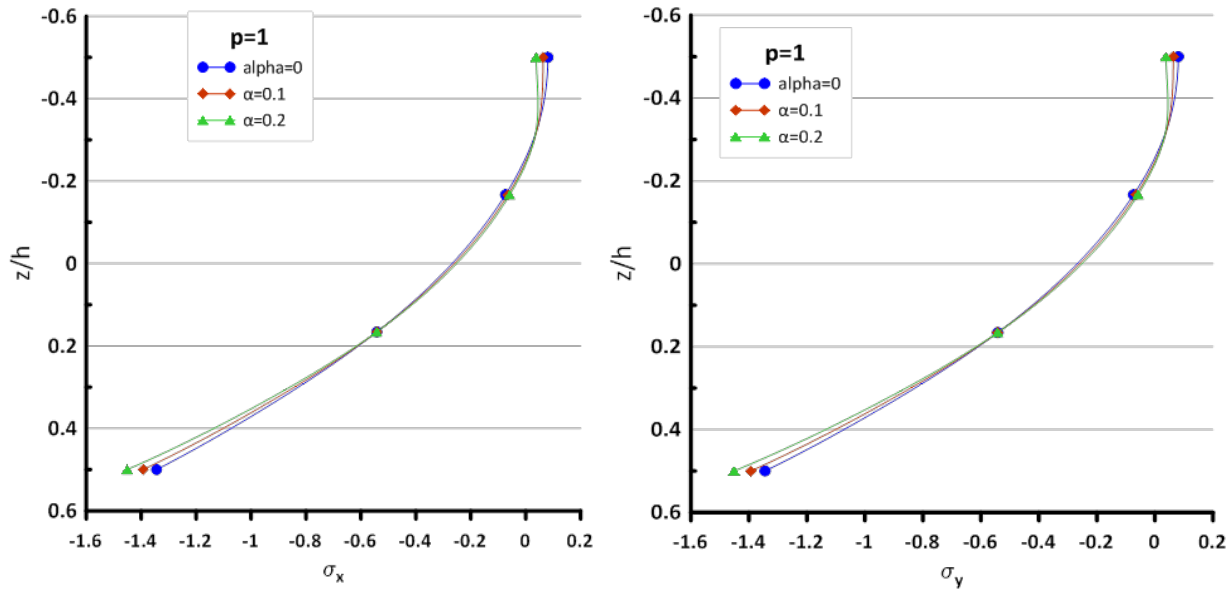

Fig. 4. Effects of the porosity distribution factor on the through-the-thickness distributions of in-plane normal stresses for FGM spherical shell (a/h=10, R/a=1)

References

[1] G. R. Kirchhoff, Uber das Gleichgewicht und die Bewegung einer Elastischen Scheibe, J. fur Reine Angew. Math. 40(1850) 51-88. https://doi.org/10.1515/crll.1850.40.51

[2] R. D. Mindlin, Influence of rotatory inertia and shear on flexural motions of isotropic elastic plates, J. Appl. Mech. 18 (1951) 31-38. https://doi.org/10.1115/1.4010217

[3] A. S. Sayyad and Y. M. Ghugal, Static and free vibration analysis of doubly-curved functionally graded material shells, Compos. Struct. 269 (2021) 1-17. https://doi.org/10.1016/j.compstruct.2021.114045

[4] B. M. Shinde and A. S. Sayyad, A new higher order theory for the static and dynamic responses of sandwich FG plates, Comput. Mech 52(1) (2021) 102-125.

[5] B. M. Shinde and A. S. Sayyad, A new higher order shear and normal deformation theory for FGM sandwich shells, Compos. Struct. 280 (2021) https://doi.org/10.1016/j.compstruct.2021. 114865

[6] Y. Q. Wang and J. W. Zu, Large amplitude vibration of sigmoid functionally graded thin plates with porosities, THIN WALL STRUCT 119 (2017) 911-924.https://dx.doi.org/10.1016 /j.tws.2017.08.012

[7] N. Wattanasakulponga and V. Ungbhakornb, Linear and nonlinear vibration analysis of elastically restrained ends FGM beams with porosities, Aerosp Sci Technol 32(1) (2014) 111-120. https://doi.org/10.1016/j.ast.2013.12.002

[8] Y. Q. Wang, J.W. Zu, Vibration behavior of functionally graded rectangular plates with porosities and moving in thermal environment, Aerosp Sci Technol 69 (2017) 550-562. https://doi.org/10.1016/j.ast.2017.07.023

[9] Y. Q. Wang, H. Wan, Y.F. Zhang, Vibration of longitudinally traveling functionally graded material plates with porosities, Eur. J. Mech. 66 (2017) 55-58. https://doi.org/10.1016/j.euromechsol.2017.06.006

[10] B. Zhu, X. C. Chen, Y. Guo, Y. Li, Static and dynamic characteristics of the post-buckling of fluid conveying porous functionally graded pipes with geometric imperfections, IJMS 189(2020) 1-57 https://doi.org/10.1016/j.ijmecsci.2020.

[11] A. M. Zenkour, Generalised shear deformation theory for bending analysis of functionally graded plates, Appl. Mathe. Modell.30 (2006) 67-84. https://doi.org/10.1016/j.apm.2005.03.009

[12] S. Dharan, S. Prakash, V. S. Savithri, A higher order shear deformation model for functionally graded plates, ICTT (2010).

[13] L. Hadji, F. Bernard, A. Safa and A. Tounsi, Bending and free vibration analysis for FGM plates containing various distribution shape of porosity Adv Mat Res.10 (2) (2021) 115-135. https://doi.org/10.12989/amr.2021.10.2.115